Complex Kinetics of Desorption and Diffusion. Field Reversal Study of K Excited-State Desorption from Graphite Layer Surfaces

Leif Holmlid[†]

Reaction Dynamics Group, Department of Chemistry, University of Göteborg, SE-412 96 Göteborg, Sweden

Received: May 27, 1998

Rapid molecular-beam kinetics data are reported of thermal desorption of K atoms from pyrolytic graphite films over the temperature range 960−1800 K. By using the so-called field reversal method (FR), the kinetics of desorption is studed at time constants down to the microsecond range, where bulk diffusion becomes rate-limiting. The neutral and ionic desorption rates are measured and shown to contain both a primary as well as a secondary rate. These measurements are combined with data on the steady-state and FR peak signals, revealing several states of K on the surface, similar to the previously studied case of Cs on pyrolytic graphite. Two covalently bound states σ_{4p} and σ_{3d} exist, which are 4.30 and 4.40 eV, respectively, below the corresponding atomic configurations 4p (a ^{2}P° term) and 3d (a ^{2}D term) outside the surface. An ionic state is also found, which is 2.0 eV below the corresponding desorbed ion K^+ (with the electron at the Fermi level). The 4s and 5s states do not correlate with stable adsorbed states. The apparent neutral rate of desorption is only slowly temperature dependent in the range 960−1550 K, with a primary (fast) rate constant of the order of 300 s^{-1} and a secondary (slow) rate of 1−10 s^{-1}. This is due to interconversion processes involving diffusion on the surface. In the range 1550−1760 K, processes with activation energies up to 6.07 eV and preexponential factors up to 10^{21} s^{-1} are observed for both the fast and the slow rates. Such large preexponential factors are indicative of thermal electronic excitation processes, implying a direct switch to a Rydberg state on the surface. The thermal emission and desorption of alkali atoms in Rydberg states is possible by two main mechanisms: by direct emission from the bulk into high Rydberg states over a thermal barrier of 7.4 eV and by excitation from the covalent states that are transferred to Rydberg states in collisions with the surface.

1. Introduction

There exist several reports on the formation of Rydberg states[1,2] of alkali atoms at high-temperature surfaces,[3−13] but the processes that give this emission have not been clear in detail. To understand the kinetics of formation of such states, we have made new experiments with the field reversal method for kinetic studies of alkali ion and atom desorption. This method has been developed both by Russian groups[14,15] and in our group[16−18] after its first correct application in 1968 by Zazula.[19] It can at present reach a time resolution of the order of tens of nanoseconds,[18,20,21] a factor of 1000 shorter than the conventional chopped beam method. In this way, desorption processes have been studied at much higher temperatures than before, providing high-resolution results especially for Cs on basal graphite surfaces.[20−22] Since this method has the potential to reach picosecond rates, it should soon be able to give true dynamic information about desorption and diffusion processes on surfaces.

The kinetics of desorption from simple surfaces might be considered a mature field, where just a few groups are active. However, the field reversal (FR) desorption method with its much improved time resolution and possibilities of simultaneous measurements of neutral and ionic desorption rates has been used in just a few cases,[14,15] and where it has been used in a more elaborate way, new and unexpected results have emerged. This is due to its ability to reach much higher temperatures where the time constants for desorption are too short for other methods. For example, in our previous studies of Cs on basal graphite surfaces, a very rapid channel for diffusion into the surface was observed[20,23] with a large preexponential factor and a very large activation energy. The thermal activation energy of 6 eV for this process is the same as for forming a Rydberg state of Cs outside the surface, i.e., equal to the sum of the desorption energy and the excitation energy. The preexponential factor in the rate constant was found to be 10^{25} s^{-1}, which is a factor of 10^{12} larger than possible for a normal desorption preexponential (which corresponds to a vibration on the surface). The reason for this very large preexponential value appeared to be that it corresponds to an electronic excitation, but the details of this excitation were not fully resolved for Cs on graphite. In the near future, it is expected that it will be possible to study the excitation processes directly by femtosecond spectroscopy, in the way recently described for Cs on a Cu(111) surface.[24]

The Cs/graphite FR kinetic studies were the starting point for the successful searches for Rydberg atoms from high-temperature surfaces that were mentioned above. In this study we present a comprehensive picture of the desorption kinetics related to the three lowest adsorbed states of K on a pyrolytic graphite layer on Ir metal. The reason for using a graphite layer on Ir instead of a graphite crystal is that the bulk diffusion gives smaller fluxes, owing to the diffusion barrier imposed by the boundary between the graphite and the metal. It has been shown that the rate of desorption is mainly determined by the graphite layer, even in cases where the graphite surface coverage is far

[†] Phone no. +46-31 7722832, Fax no. +46-31 7723107, E-mail Leif.Holmlid@phc.chalmers.se.

10.1021/jp9823796 CCC: $15.00
Published on Web 12/08/1998

from complete.[22] One state of K on the surface is ionic and mobile, and two states are covalently bound on the surface. These covalent states desorb to the 4p and 3d states of K outside the surface. Their potential energy curves cross adsorbed Rydberg state potentials outside the surface, and in this way nearly desorbing K atoms can be transferred into Rydberg states on the surface after collisions with the surface. This is believed to be the main mechanism for the desorption of Rydberg species of alkali atoms from graphite surfaces, which has been observed and reported in a large number of publications from our group. The direct emission into very high Rydberg species during diffusion out from the bulk of the graphite is also feasible and observed in the present experiments.

2. Surface Ionization Theory

Surface ionization as formulated in the Saha-Langmuir equation[14,25,26] governs the fluxes of ions and neutrals that leave the surface in thermal equilibrium. In the present case, this means that both neutral atoms K and ions K^+ desorb from the surface, in proportions determined by statistical mechanical theory. The degree of ionization α (ratio of numbers of ions desorbing from the surface and numbers of corresponding neutrals) is given by the Saha-Langmuir equation, which for alkali atoms is

$$\alpha = i_+/i_0 = {}^1/_2 \exp(e(\Phi - I)/kT) \tag{1}$$

where i_+ is the current density from the surface, i_0 is the neutral flux density in current units measured with an accelerating electric field, e is the unit charge, Φ is the work function of the surface, I is the ionization potential of desorbing atoms, k is the Boltzmann constant, and T is the surface temperature. The value of α is larger than $^1/_2$ only if $\Phi > I$. It is also convenient to define the coefficient of ionization β as usual as

$$\beta = \alpha/(1 + \alpha) \tag{2}$$

The degree of ionization α can also be derived by kinetic reasoning, using the relations

$$i_0 = k_0 n \quad \text{and} \quad i_+ = k_+ n \tag{3}$$

where i_0 and i_+ are the flux densities of atoms and ions respectively from the surface, n is the surface density of the adsorbed species, and k is the rate constant for desorption from the surface for the respective particle. In this formulation

$$\alpha = k_+/k_0 \tag{4}$$

is found to be valid. Assume now that we have a constant flux density f impinging on the surface, for example, in the form of a molecular beam. At steady state (above a certain transition temperature), and with the electric field outside the emitter accelerating (indicated >) or retarding (indicated <), one obtains

$$f = i_+ + i_0 = k_+ n_> + k_0 n_> \tag{5}$$

$$f = i_0 = k_0 n_< \tag{6}$$

In the time-dependent case, which is the case of most interest here (see also ref 15), the rate equations for desorbing ions and atoms are

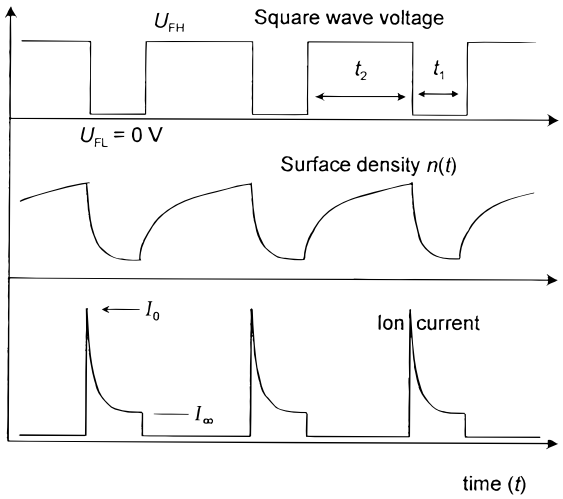

Figure 1. Extraction function of the FR apparatus. The top curve shows the square wave applied to the FR slit, and the second curve shows the time variation of the surface density. The third curve shows the FR signal due to the desorbing ions during the accelerating time intervals, with zero signal during the retarding time intervals.

$$\frac{dn_>}{dt} = f - k_+ n_> - k_0 n_> = f - k_> n_> \tag{7}$$

$$\frac{dn_<}{dt} = f - k_0 n_< = f - k_< n_< \tag{8}$$

In the FR scheme, the electric field outside the emitter surface is switched periodically between accelerating and retarding. The resulting surface density and ion current variations in time are depicted schematically in Figure 1. Equations 7 and 8 have the solutions[18]

$$n_>(t) = n_>(0) \exp(-k_> t) + \frac{f}{k_>}(1 - \exp(-k_> t)) \tag{9}$$

$$n_<(t) = n_<(0) \exp(-k_< t) + \frac{f}{k_<}(1 - \exp(-k_< t)) \tag{10}$$

The relations between $n_>(t)$ and $n_<(t)$ at the times t_1 (L $\rightarrow$ H, i.e., accelerating to retarding field) and t_2 (H $\rightarrow$ L, i.e., retarding to accelerating field) give the final surface densities. Since the flux densities are given generally by

$$i(t) = kn(t) \tag{11}$$

one finds

$$i_>(t) = f + \alpha f \exp(-k_> t) \frac{1 - \exp(-k_< t_2)}{1 - \exp(-k_> t_1 - k_< t_2)} \tag{12}$$

$$i_<(t) = f - \beta f \exp(-k_< t) \frac{1 - \exp(-k_> t_1)}{1 - \exp(-k_> t_1 - k_< t_2)} \tag{13}$$

From $i_>(t)$, one can easily find the ion flux density

$$i_+(t) = \beta i_>(t) \tag{14}$$

Introducing the two values $I_0 = i_+(0)$ and $I_\infty = i_+(\infty)$, one finds from eq 12 the ratio between the FR peak and the final dc level of the signal with large acceleration time t_1

$$\frac{I_0}{I_\infty} = 1 + \alpha \frac{1 - \exp(-k_< t_2)}{1 - \exp(-k_> t_1 - k_< t_2)} \quad (15)$$

For $t_2 \rightarrow \infty$, this expression becomes equal to $1 + \alpha$, and thus the ratio between the FR peak value at time t_2 and at infinite retardation time becomes

$$\frac{I_0(t_2)}{I_0(\infty)} = \frac{1 + \alpha \dfrac{1 - \exp(-k_< t_2)}{1 - \exp(-k_> t_1 - k_< t_2)}}{1 + \alpha} \quad (16)$$

In general the FR kinetics method has several unique advantages, as also mentioned above. Especially the variation of the pulse lengths provides a very powerful method to disentangle the complex kinetics. In the experiments presented here, the accelerating time was varied from 400 μs to 100 ms, and the retardation time from 80 μs to 5s. This meant resolution of time constants over at least 4 decades in the same experiment. Thus, it is possible to determine many rate constants from the measurements and to resolve them into their parameters, the activation barriers and preexponentials.

3. Experimental Section

The experiments were carried out in a HV apparatus with a base pressure of 5×10^{-7} mbar during the experiments. A thermal K beam effuses out from a two-chamber source, with the reservoir at approximately 480 K and the front of the source at 510 K. The source chamber is separately pumped to decrease the gas load in the HV chamber. The distance from the source to the emitter studied is 0.9 m. This means that the beam gives a constant pressure at the sample of the order of 10^{-10} mbar. The pumping speed from the diffusion pumps in the chamber with the sample is 3000 dm^3/s.

As the emitter an Ir foil with a thickness of 50 μm and dimensions 25×4 mm was used. The Ir foil was covered by a graphite layer at a surface temperature of 1550 K by admission of ethylene gas at a pressure of 10^{-5} mbar, until the electron emission reached a high and stable value, indicating a work function in the range 4.3−4.4 eV. It is known[27] that the structure of the surface can vary with the conditions during its preparation and later treatment. Under the conditions used here, a two-dimensional graphite film is formed. The kinetic studies performed are very sensitive to the surface conditions, and drifts in the surface conditions are easily observed, as for example after prolonged heating at temperatures close to 2000 K. For this reason, the graphite layer was renewed periodically, often after cleaning the surface by oxygen admission to a state with no adsorbed carbon. The reason for using graphite on Ir instead of a homogeneous graphite crystal is the smaller amount of bulk diffusion, which limits the useful temperature range for the graphite crystal. The graphite/Ir system has been studied extensively by other groups; see, for example, ref 27. The surface is very stable under most conditions, and its properties are virtually unchanged even after exposing the sample to the ordinary atmosphere. The emitter was heated by passing an ac current through it. Its temperature was measured with an optical pyrometer through a large window facing the back side of the emitter. No emissivity corrections were made owing to the large emissivity of carbon. The K beam reached the surface along the normal of the foil surface.

The emitter was mounted in a small ion source, with a FR slit to which a square wave potential is applied. It should be noted that it is considered impossible to use meshes in the electrodes to reach more homogeneous field strengths, since Rydberg species will not be able to pass through the mesh openings.[28−32] A vertical cut through this part of the apparatus is shown in Figure 2. Two standard values for the emitter voltage are used, 9 and 40 V, corresponding to field strengths of approximately 20 and 80 V cm^{-1}. The ions leaving the foil sample and the ion source are accelerated by a negative slit, the accelerator slit. This slit acts as a shielded feedthrough for passage through the vertical Cu plate, which isolates the FR ion source part from the detector part. The ions are deflected toward the multiplier in the upper part in Figure 2 by a static quadrupole.[33] They are accelerated by −4.5 kV on the dynode and impact there, giving secondary electrons that are attracted by the grounded scintillator.[18] The light from the scintillator is amplified by the photomultiplier (PM in Figure 2), and the current signal is observed on an oscilloscope. The loading resistor is 10 kΩ or less to decrease the rise time of the measurements.

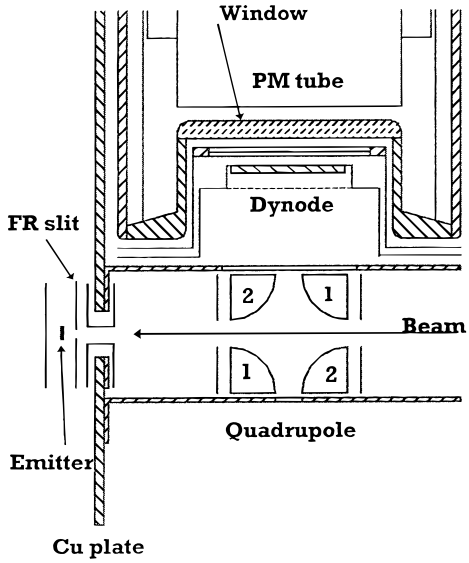

Figure 2. Field reversal kinetics apparatus: vertical cut through the ion source and detector part of the apparatus. The ions leave the emitter region through the FR slit and pass through the double-sided accelerator slit, which covers the opening through the Cu plate that carries the ion source and ion optics parts. The quadrupole consists of four quarter-cylindric rods in the horizontal direction. The scintillator is mounted between the dynode and the window.

The voltage applied to the FR slit is a square wave with its high voltage at a variable value between 0 and 70 V, and the low voltage at ground. The times at the low-level t_1 (ion acceleration time) and at the high-level t_2 (ion retardation time) can be varied independently between several seconds and less than a microsecond. The rise and fall times are <10 ns.[18] How the time variation of the external field influences the surface density on the emitter surface is discussed in the preceding section.

The work function of the C/Ir emitter surfaces has been studied by measurements of the effective and Richardson work functions from the thermal electron emission and is found to vary between 4.25 and 4.50 eV. In the literature, values of 4.4−4.5 eV are usually reported on C on Ir.[27] In previous studies from our group a value of 4.5 eV is reported for the basal graphite surface.[20,21] A detailed study of a graphite layer on Pt(8%W)[34] showed that the work function varied with temperature in a nonlinear way, in the range 4.35−4.55 eV at temperatures 1000−1750 K. In the present studies, the Richardson work function is 4.36 ± 0.07 eV at $U_{em} = 9$ V and 4.50

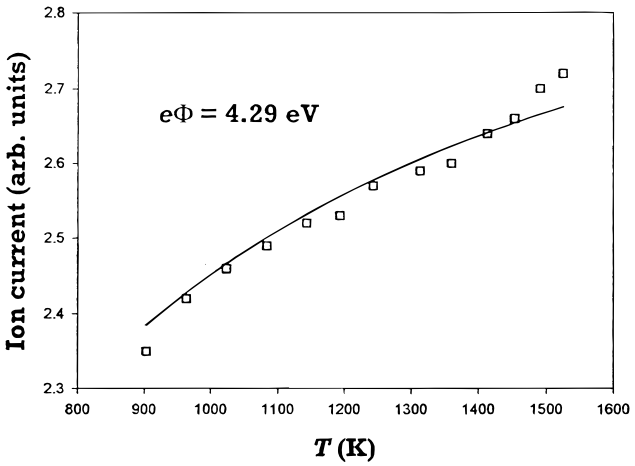

Figure 3. K^+ ion current as a function of sample temperature with a constant beam under steady-state conditions. The points are measured, while the curve is calculated from the Saha-Langmuir equation, eqs 1 and 2, with a work function of 4.29 eV. The electric field strength was 20 V cm^{-1} outside the sample; i.e., the sample was at a voltage of 9 V.

$\pm$ 0.08 eV at $U_{em} = 40$ V. The effective work function is, however, lower also in the case of $U_{em} = 40$ V, namely, 4.27 eV. As discussed below, the steady-state surface ionization experiments also indicate a work function of approximately 4.3 eV. Since the same work function is found with surface ionization and in electron emission, the surface inhomogeneity should be rather small.[14] The kinetic experiments give values of the degree of ionization α, and thus of the work function, in good agreement with the values discussed here.

The flux density of the beam at the emitter surface was 2×10^{-9} to 2×10^{-8} A cm^{-2} or 1×10^{10} to 1×10^{11} cm^{-2} s^{-1}. This means that if the smallest rate constant observed here, 1 s^{-1}, was a desorption rate constant, the surface density would be 10^{-4} of a monolayer. At this low surface coverage, no substantial influence on the work function is expected. In general, the dominating desorption rate constant is much larger than 1 s^{-1} even at the lowest temperature used, around 1000 K. The results reported below for example on the steady-state surface ionization show that the work function is not decreased by K surface coverage in the temperature range studied.

4. Results

4.1. Ion Signal Temperature Variation. The steady-state ion signal is shown in one example in Figure 3, with an electric field strength of 20 V cm^{-1}. The Saha-Langmuir equation in the time-independent form of eq 14 is directly applicable, with the coefficient of ionization given by eqs 1 and 2. Neither the neutral nor the ionic desorption rates need to be explicitly included to make a comparison between theory and experiments, as shown in Figure 3. Instead eq 1 can be used directly to give the work function from the temperature dependence of the signal. This treatment assumes that there is no large signal flux directly from the bulk, since the basic assumption for the theoretical development is that eq 5 is fulfilled. At high temperature, the background from the K preabsorbed in the bulk increases strongly, as seen in the figure, which does not agree with eq 5. Thus, measurements of the steady-state current above 1500 K cannot be used to determine the work function. The theoretical curve shows the variation expected for a work function of 4.29 eV using eq 1, thus slightly lower than the ionization potential of K, which is 4.34 eV. The results of this type show that the Saha-Langmuir equation is fulfilled under steady-state conditions, and thus that the energy levels involved

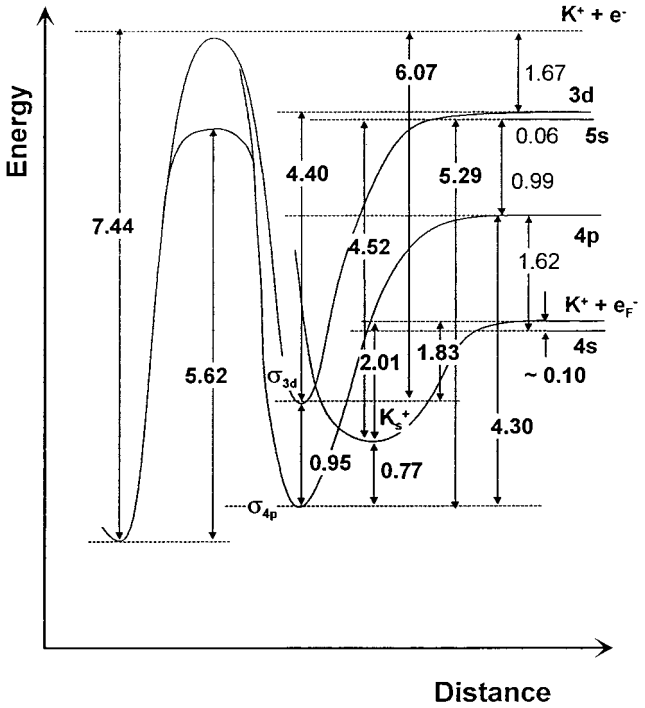

Figure 4. Schematic potential energy curves with activation energies in eV for the interaction of K with a C/Ir surface. To the right, the spectroscopic values of the energy differences between the states are given.

with accelerating field are K(4s) and $K^+ + e_F^-$, with a difference in energy of 4.34−4.29 eV = 0.05 eV and with the $K^+ + e_F^-$ level higher in energy.

The kinetics of *ion* desorption is complex owing to the number of states on the surface involved, and outside the scope of the present study. Under some conditions ($T < 1400$ K and short retardation times, e.g., $t_1 = 0.4$ ms, $t_2 = 80$ μs), a preexponential factor can be found that is large enough to be considered to be a true desorption preexponential. The result is a barrier for ion desorption (from the state K_s^+ to $K^+ + e_F^-$) of 2.01 $\pm$ 0.01 eV and a preexponential of 3.7×10^{12} s^{-1}. This desorption energy is included in Figure 4 and in Table 1.

4.2. Diffusion from the Bulk. The first method to use to disentangle the complex kinetics due to several adsorbed states on the surface is to study the desorption of preabsorbed K in the bulk. This was very useful in the case of Cs/C system.[20,21] The preabsorption takes place at high temperature and with retarding electric field. Under these conditions, the diffusion into the bulk is very rapid and goes over a high barrier in the surface, as demonstrated directly in ref 13. (No difference in the diffusion behavior for the pyrolytic graphite crystal used in ref 13 and the pyrolytic graphite layer studied here has been observed.) The density of K is very small in the graphite layer, still far from any intercalation compound. With no impinging beam it is difficult to directly apply the formulas in the theoretical section above, since the flux density to the surface is not constant but varies with temperature. Further, the flux does not reach the same adsorbed state on the surface as if the flux was coming from an external flux (the K beam), like in the Cs/C system. The result for the temperature variation of the steady-state ion current from the sample is the same at field strengths at 20 and 80 V cm^{-1}, namely, a barrier of 7.44 $\pm$ 0.06 eV in the temperature range 1500−1700 K. Below 1400 K, the signal is too small relative to the multiplier dark current to be measured reliably. Since the difference $e(\Phi - I)$ is small as shown above, there is no need to correct the observed barrier

TABLE 1: Activation Barriers and Rate Parameters for the Data Included in Figure 4

activation barrier (eV)	measured values (eV)	preexponential factor (s^{-1})	measurement	beam	data in Figure no.
7.44	7.44 ± 0.06		$I_\infty = I$(steady state)		5
6.07	6.08 ± 0.19	8.2×10^{20}	$I_0(k_<, k_>)$	yes	8
	5.93 ± 0.24	4.3×10^{20}	$I_0(k_<, k_>)$	yes	9
5.62	5.62 ± 0.07		I_0		5
5.29	5.33 ± 0.21	1.0×10^{20}	$I_0(k_<, k_>)$	yes	9
4.52	4.70 ± 0.21		I_∞	yes	13
4.40	4.40 ± 0.31	6.2×10^{16}	$I_0(k_<, k_>)$	yes	8
4.30	4.40 ± 0.16		I_0		in text
2.01	2.01 ± 0.01	3.7×10^{12}	$k_>$	yes	in text
1.83	1.73 ± 0.12	1.2×10^{9}	$k_>$		12
0.95	0.93 ± 0.35	1.2×10^{4}	$I_0(k_<, k_>)$	yes	8
	1.47 ± 0.31		I_0(fast)/I_0(slow)	yes	11
0.77	0.78 ± 0.27	7.3×10^{3}	$I_0(k_<, k_>)$	yes	9
	−0.80 ± 0.18	0.77	$I_0(k_<, k_>)$	yes	9
	0.68 ± 0.11		I_0(fast)/I_0(slow)	yes	10

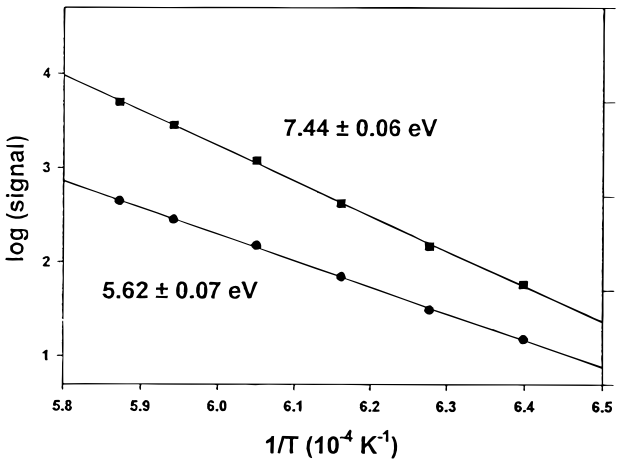

Figure 5. Temperature variation of the ion current I from the sample, with K beam interrupted (beam flag closed), and of the FR peak signal I_0, measured simultaneously. The energy barriers are given in the figure. The sample voltage was 9 V, and the accelerating electrode was at −229 V. During the FR measurement, $t_1 = 0.4$ ms and $t_2 = 5$ ms were used.

for the temperature variation of β, as had to be done in refs 20 and 35. As in that case, the peak of this barrier (which is the largest measured for this system) is placed at the ionization limit $K^+ + e^-$. The adsorbed state in the bulk inside this barrier is taken as being close in energy to and probably somewhat lower than the lowest adsorbed state for K on the surface. See further Figure 4 and Table 1.

By FR switching, the ion peak signal I_0 is obtained as a function of temperature. This measurement has been performed with 80 V cm^{-1} field strength, giving a barrier of 5.62 ± 0.07 eV in the range 1560−1700 K, as shown in Figure 5. In the present experiment, $t_1 \ll t_2$ was used. This means that the FR peak signal I_0 does not increase as rapidly with temperature as the steady-state current I_∞. Following eq 15, this is clearly the case when the work function and the degree of ionization α both are large, and in this case it follows directly from eq 15 that the work function is 6.1 eV. This is a much too high work function to be found in the present system: even an Ir surface with no carbon coverage has a work function of only 5.2 eV, so this is obviously not the explanation for these results. In the case with a temperature-dependent flux from the bulk to the surface, I_0 is a measure of the amount of K accumulating on the surface with retarding field, which is then sampled during the short period with accelerating field. Thus, there exists a barrier for transport out from the bulk with this barrier that belongs to the rate-controlling step in the case with retarding field. This barrier is slightly below the 5s level; in fact, they agree within error limits. The reason why the higher barrier of 7.44 eV is not observed also for the I_0 temperature dependence is that with retarding field, the high Rydberg states will not be emitted from the bulk owing to the external field. It has been shown[36] that the FR peak I_0 is due to Rydberg species accumulating outside the surface during the retarding phase, and it is possible that the reason for the 5.62 eV barrier to become observable is the possibility for the K atoms from the bulk to form long-lived excited species by the interaction with the 5s and the adjacent 3d levels.

Under different FR conditions using long times t_1 and t_2 (0.1−0.2 s), the temperature variation of the FR peak gives an activation barrier of 4.40 ± 0.16 eV, measured between 1540 and 1700 K for both high and low field strengths. (The accelerating electrode was at −220 V). From eq 15, the FR peak I_0 is in this case equal to (1 + α) times the signal I_∞, since the times t_1 and t_2 are large. The large FR peaks observed would indicate a very large α. If α is larger than 0.5, it should decrease with increasing temperature, but the opposite is found here. The only possibility to apply the surface ionization description is then that it is I_∞ which varies with a barrier of 4.40 eV. A rapid variation of I_∞ of the required size was also seen in the experiment, but the barrier value was difficult to obtain accurately owing to a too low signal, so the I_0 value is relied on instead. The barrier observed should correspond to the rate-determining step in the process of emission and desorption from the bulk, and since it is lower and found under different FR conditions than the 5.62 eV barrier described above, it should correspond to the desorption process from the surface. It is highly unlikely that such a large desorption energy can correspond to desorption of a ground-state atom since the adsorbed state would be a very deep lying level. In Figure 4 this desorption barrier thus connects the lowest covalent state, which might be designated σ_{4p}, to the 4p desorbed state. In Figure 4, this energy is a 4.30 eV. See also Table 1. An alternative (and possibly parallel and simultaneous) process is from the higher covalent state σ_{3d} to the desorbed state 3d, shown with an energy barrier of 4.40 eV in Figure 4. These states give ion emission since they are transferred in collisions with the surface into Rydberg states, which are then field ionized. The reason why the desorption does not lead directly to ions K^+ outside the surface is that the transfer from the covalent states to the ionic adsorbed state is required for this process, and this transfer is too slow.

4.3. Neutral Rates of Desorption. The measurements with the beam cut off have thus defined the main energetics for this desorption system. The next kind of results needed is the neutral

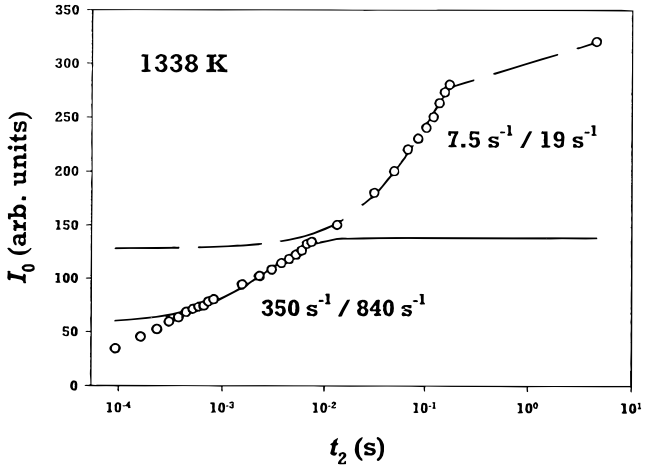

Figure 6. FR peak signal as a function of the retardation time t_2, at a surface temperature of 1338 K. The emitter was at 9.3 V, the FR voltage at 29 V, and the accelerating voltage at −219 V. The accelerating time t_1 was close to 100 ms. The fit of the fast rate is shown in the bottom curve, and eq 16 was used for this calculation. The limiting value $I_0(\infty)$ is chosen to be 138 au to the fit the results, and the rate constants are found to be $k_< = 350$ s^{-1} and $k_> = 840$ s^{-1}. The slow rate is found from the fit in the top curve, giving $k_< = 7.5$ s^{-1} and $k_> = 19$ s^{-1} with the measured limiting value of 320 au. The degree of ionization α is 1.4−1.5 in the fits, indicating a work function of 4.46 eV.

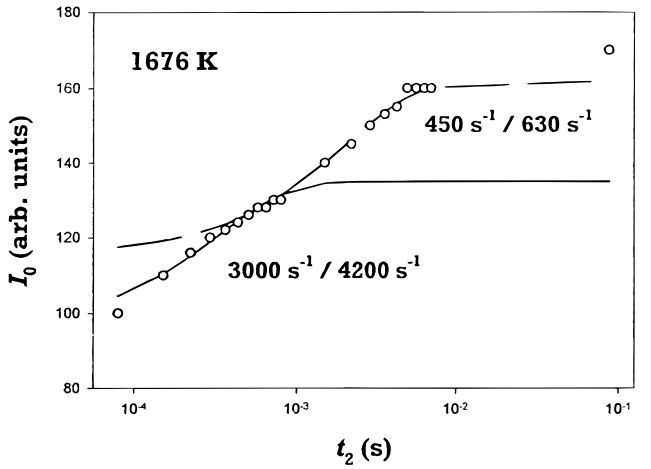

Figure 7. FR peak signal as a function of the retardation time t_2, at a surface temperature of 1676 K. See further Figure 6. The data used for the fast rate are $I_0(\infty) = 135$ au, $k_< = 3000$ s^{-1}, and $k_> = 4200$ s^{-1}, and for the slow rate $I_0(\infty) = 162$ au, $k_< = 450$ s^{-1}, and $k_> = 630$ s^{-1}. The degree of ionization α is 0.4 in both fits, which gives a work function of 4.21 eV.

rate of desorption determined with a K beam striking the emitter surface. It can be found from the FR peak height and its variation with the retarding period, in the way described by eq 16. The same method was used in ref 21 in the case of Cs/C. As in that case, the I_0 variation with t_2 is determined by two consecutive rate constants, which are named fast and slow, respectively. It is possible to determine the break point between the two parts of the curve by inspection, or by trying to fit a single rate constant to the data. In the present measurements, the electric field strength was always 20 V cm^{-1}. Examples of the results and the corresponding fits to a fast and a slow rate are given in Figures 6 and 7. Good fits are obtained below 1500 K by using the limiting signal value from the fast rate as the starting point for the slow rate, as seen in Figure 6. This means that the signal due to the steady-state surface density determined by the beam flux density and the neutral rate of loss is the starting point for the slow rate, which is just added on this first limiting density.

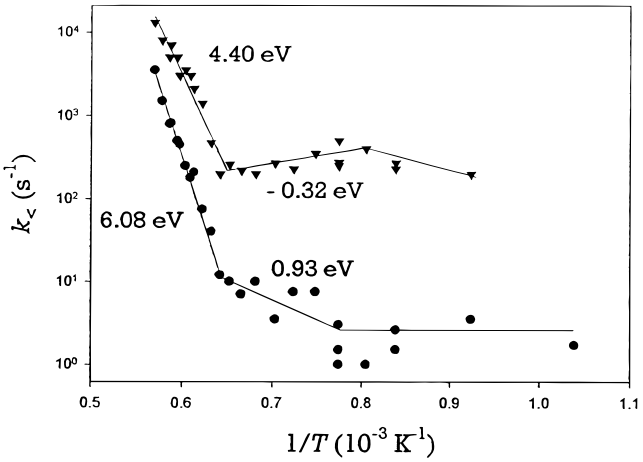

Figure 8. Rate constant $k_<$ from measurements of the neutral desorption with examples in Figures 6 and 7, as a function of temperature. The fast rate is shown at the top of the figure, and the slow rate at the bottom. The activation barriers, etc., are given. The rate parameters are $E = 4.40 \pm 0.31$ eV, $A = 6.2 \times 10^{16}$ s^{-1}; $E = -0.32 \pm 0.10$ eV, and $A = 19$ s^{-1} for the fast rate, $E = 6.08 \pm 0.19$ eV, $A = 8.2 \times 10^{20}$ s^{-1}; $E = 0.93 \pm 0.35$ eV, and $A = 1.2 \times 10^4$ s^{-1} for the slow rate.

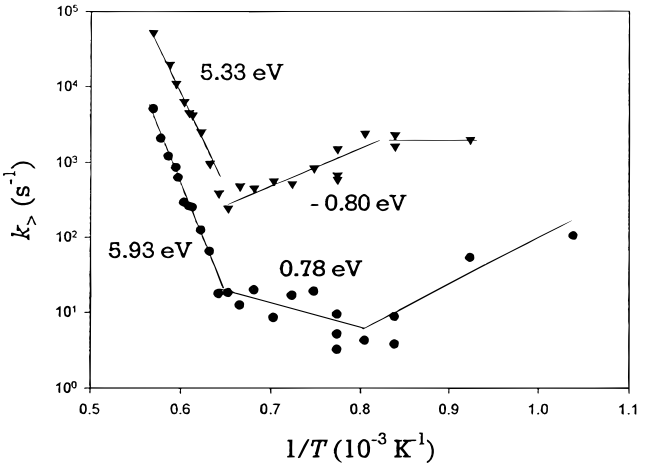

Figure 9. Rate constant $k_>$ from measurements of the neutral desorption with examples in Figures 6 and 7, as a function of temperature. The fast rate is shown at the top of the figure, and the slow rate at the bottom. The activation barriers, etc., are given. The rate parameters are $E = 5.33 \pm 0.21$ eV, $A = 1.0 \times 10^{20}$ s^{-1}; $E = -0.80 \pm 0.18$ eV, and $A = 0.77$ s^{-1} for the fast rate, $E = 5.93 \pm 0.24$ eV, $A = 4.3 \times 10^{20}$ s^{-1}; $E = 0.78 \pm 0.27$ eV, and $A = 7.3 \times 10^3$ s^{-1} for the slow rate.

At temperatures above 1500 K, the situation is somewhat more complex, as seen in Figure 7. The behavior with the slow signal on top of the fast signal can be understood if it is assumed that the state into which the beam atoms fall when approaching the surface is coupled to another state on the surface. This will be treated in detail in the Discussion section.

By varying the retardation time t_2 over a large range (3−5 decades) at given surface temperature, the rate constants, both fast and slow, can be determined from the FR peak. In the fits, both $k_>$ and $k_<$ are determined, as seen in eq 16. The temperature variation for $k_<$ is shown in Figure 8 will all the rate parameters given in figure caption, while the temperature variation for $k_>$ is shown in Figure 9. (See further in the next section.) The results are also included in Table 1. The fast and slow rates for both rate constants depend only slowly on temperature below 1500 K. The preexponential factors are very small, with time constants in the second to millisecond range. The fits are more

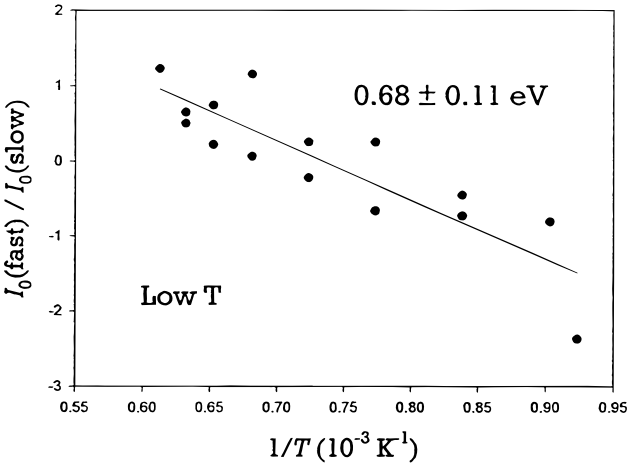

Figure 10. Ratio between the asymptotic signals in the fast and slow rates in the neutral desorption, from data of the type in Figures 6 and 7, at low temperature.

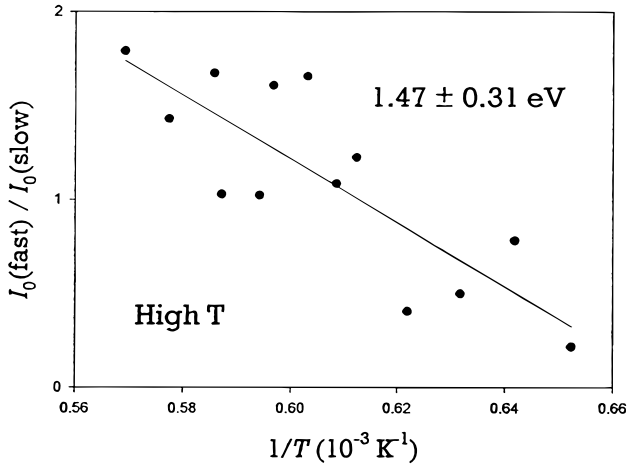

Figure 11. Ratio between the asymptotic signals in the fast and slow rates in the neutral desorption, from data of the type in Figures 6 and 7, at high temperature.

sensitive to the values of $k_<$, which is the main rate constant determined in this way. At high temperatures, above 1500 K, the fast rate for $k_<$ shows a barrier of 4.40 ± 0.31 eV, with the preexponential 6.2×10^{16} s^{-1}, while the slow rate varies with an activation energy of 6.08 ± 0.19 eV, with the preexponential factor 8.2×10^{20} s^{-1}. Between 1250 and 1500 K, the slow rate gives a barrier of 0.93 ± 0.35 eV, which is interpreted to correspond to the energy difference between the two states on the surface. See further below.

The interpretation of the rates with small barriers is that they correspond to diffusion on the surface and a related, and thus relatively slow, transformation between different adsorbed states on the surface. The large barriers have another interpretation. The slow rate, with a preexponential close to 10^{21} s^{-1}, is due to a direct switch between two different electronic states, as will be discussed below, and is interpreted in the same way as the similar rates in the case of Cs/C,[20,21] i.e., as a switch to a Rydberg state followed by fast diffusion into the bulk over a large barrier or possibly to desorption as an excited atom. This process is thought to go from the covalent σ_{3d} to the ionization limit, which in Figure 4 is shown to correspond to a barrier 6.07 eV, thus agreeing within error limits with 6.08 ± 0.19 eV. The fast rate in the same range may be from the lower covalent state σ_{4p} to the desorbed state 4p, with a barrier according to Figure 4 of 4.30 eV. The large value of the preexponential for this desorption process found here could indicate an intermixing of an intermediate state[20,37] and would thus indicate that the process is mainly desorption from the lower covalent state with some participation, via equilibrium, of the upper covalent state shown in Figure 4.

The asymptotic size of the signal that corresponds to the fast and the slow rate constants, respectively, is found from the fits to the data of the type shown in Figures 6 and 7, as also given in the figure captions. The ratio between signal contributions to the fast and slow rates I_0(fast)/I_0(slow) varies with temperature, such that the fast rate contribution dominates at high temperature. Since the contributions to the signal level of I_0 are proportional to the number of atoms that can exist in a certain state on the surface with retarding field, a larger size means a smaller rate of loss from this state. An Arrhenius plot of the ratio gives a slope of 0.68 ± 0.11 eV at low temperature, below 1600 K, as seen in Figure 10, and 1.47 ± 0.31 eV between 1600 and 1800 K (Figure 11). The first energy difference corresponds to the difference between the two lowest adsorbed states on the surface at 0.77 eV in Figure 4, while the second value corresponds to an activation barrier somewhat larger than, but related to, the energy between the two covalent states, at 0.95 eV in Figure 4. These identifications are also included in Table 1. The reasons for these identifications will be discussed below.

4.4. Ion Desorption Kinetics. The results in Figure 9 on ion desorption were obtained from the measurements of I_0 as a function of t_2 with examples given in Figures 6 and 7. Below 1600 K, the fast rate varies with −0.80 eV; i.e., it decreases with increasing temperature. Since the ions are emitted from the ionic state on the surface, the negative temperature dependence indicates a decreased rate of loss from the ionic state, probably by transfer via diffusion from the lowest covalent state σ_{4p}. The slow rate that shows approximately equally large but positive temperature variation should then signify the transfer in the other direction. Above 1600 K, the fast rate with the energy barrier of 5.33 ± 0.21 eV shows the desorption from the lowest covalent state σ_{4p} to the state 5s outside the surface, at 5.29 eV in Figure 4. The slow rate in this case is almost the same as the slow rate for neutral loss, namely, from the σ_{3d} state on the surface to the Rydberg limit.

A few results from separate ion desorption experiments must also be reported to complete the picture. Of special interest is the ion desorption kinetics with the K beam interrupted, shown in Figure 12 in a case with long t_1 and t_2. The low preexponential factor, 1.2×10^9 s^{-1}, indicates that this process is not directly from the ionic state on the surface, but more likely from one of the covalent states that is filled from the K atoms in the bulk. The relatively low activation barrier of 1.73 ± 0.12 eV indicates that the desorption takes place from the upper covalent state to the desorbed ionic state. In Figure 4 the corresponding barrier of 1.83 eV is placed between the upper covalent state σ_{3d} and the $K^+ + e_F^-$ level. This result thus fixes the relation between the upper covalent state σ_{3d} and the desorbed ion state. See also Table 1.

No similar kinetic results exist for direct ion desorption from the lower covalent state. However, the results for ion desorption (to be published) support strongly the placement of this level as in Figure 4. The position of the lowest covalent state relative to the other states is also given by the rates described above, giving the energy difference 5.29 eV to the 5s level outside the surface. There also exist more results on the temperature dependence of the signal I_∞ with a K beam above 1500 K, as shown in Figure 13 with two different voltages of the accelerating slit and short time t_1 and t_2. The slope found gives a barrier

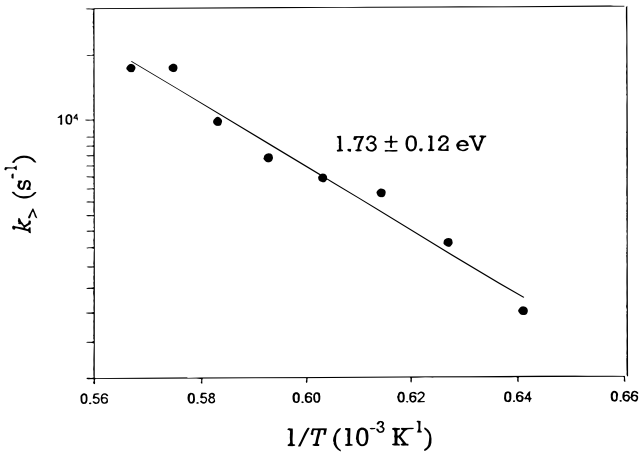

Figure 12. Ionic rate of desorption with FR kinetics with K beam interrupted (beam flag closed). The slope of the line gives $E = 1.73 \pm 0.12$ eV and $A = 1.2 \times 10^9$ s^{-1}. The rate constant was found from the 90%−10% fall time of the signal. The sample voltage was 9 V, the FR voltage was 29 V, and the switching times were $t_1 = 0.11$ s and $t_2 = 0.17$ s.

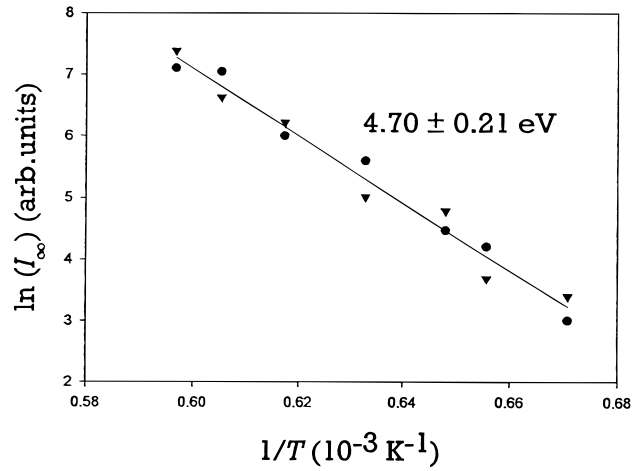

Figure 13. Temperature variation of the signal I_∞ from the sample, with K beam on. Data with voltages −15 and −150 V on the accelerating slit are included, which shows that no focusing problems exist in this case. The energy barrier is given in the figure. The sample voltage was 8.8 V, the FR voltage was 27 V, and the switching times were $t_1 = 3.7$ ms and $t_2 = 3.7$ ms.

of 4.70 ± 0.21 eV for this signal, which must correspond to emission into an ionic state above the ordinary ionic state. It is obvious that the passage from the ionic state K_s^+ on the surface to the desorbed ion state $K^+ + e_F^-$ is not possible in this case. The barrier is included as 4.52 eV in Figure 4 and Table 1 and corresponds to emission into the state 5s. This state was found to give mainly ion emission in the experiments described above (with a barrier of 5.29 eV).

5. Discussion

5.1. Connected States. From the results described above one can draw one important conclusion concerning the relations between the various states on the surface and in the gas phase outside the surface. It is clear that the covalent states on the surface give almost exclusively neutral (atomic) desorbing species. However, the neutral species are highly excited and may easily be transferred to field ionizable states by collisions with the surface. This behavior on the graphite surface is different from that on a metal surface, where the ionic and neutral states are mixed into one state with a partial transfer of the electron to the surface, and the adsorbed state gives both atoms and ions in desorption, in a way consistent with (but not described by) surface ionization theory. In the picture of the desorption from graphite shown in Figure 4, several more states certainly exist, but only the few most important ones for the experimental results have been included in the present description. It should be observed that no more states outside the surface exist below the 3d state, but a multitude of states (configurations) exist between 3d and the ionization limit. Most of these higher states have large n and also large l quantum numbers, and many of their potential minima are located below the 3d level. Their interaction with the surface has been proposed[9] to give rise to long-lived states oscillating on the average at a large distance from the surface. Such states are thought to take part in the transformation of the desorbing states σ_{4p} and σ_{3d} into field ionizable states that are observed in many experiments.[3−13]

From the form of the various orbitals, it seems likely that the surface adsorbed σ_{4p} is bound to one graphite carbon p orbital, while the state σ_{3d} could be bound in a bridging position to two carbon p orbitals. This could be the reason why 3d is bonded with approximately the same energy to the surface as the 4p, despite the higher energy of the 3d state. In a somewhat naive molecular orbital picture, it is likely that these states are σ bonded, which gives a rather small ionic contribution. On the contrary, an s state, like 4s and 5s included in the discussion here, will be strongly distorted by the surface, and it is likely that atoms in such states become ionized outside the surface and that an ionic bond is formed during impact on the surface. The 4s state is probably reached during desorption from the ionic adsorbed state K_s^+, at least at higher field strengths, but the behavior of the 5s is more disputable. Since this state is far above the Fermi level in the graphite, it is conceivable that the electron in this state moves directly into the empty levels in the surface and that an ion is formed during impact, at some distance from the surface. This means that no bound state connected to 5s exists on the surface. However, the 5s could of course still be formed during desorption. It is possible that σ_{3d} during desorption may be transferred to 5s and then rapidly ionized, giving an ion free to leave the surface, and that this constitutes one way of forming ions K^+ in the thermal desorption. The results in Figures 4 and 13 are in agreement with this.

It also possible that antibonding orbitals for the K interaction with the graphite surface exist. If this is the case, thermal excitation to such states may increase the rate of desorption. If such a repulsive state existed for the 4s configuration, for example, considerable inelastic or elastic scattering should be observed. In ref 13, there is no indication of any scattering with an accelerating field for K^+ ions from the graphite, but in the case of a retarding field, some specular scattering seems to exist. This observation could be interpreted as showing the transfer from the repulsive state to the ionic state K^+ outside the surface with accelerating field, which would force the ions out in the normal direction, and a scattering from this repulsive state in the case of a retarding field. However, it is not yet possible to state anything conclusively about the possibility that such states are of importance for the thermal desorption processes discussed here.

5.2. Processes Involved in the Neutral Desorption. The main time dependence of the neutral desorption is similar to the case of Cs/C reported in refs 20 and 21. This is so, especially in the respect that the dependence on the retardation time has two time constants that behave independently, in the way shown in Figures 6 and 7. This means that the surface density, sampled

by the FR peak height, increases from small retardation times up to the limit set by the fast rate constant in the expected exponential form but that the surface density then continues to increase beyond this limit, toward a new limit set by the slow rate constant. This behavior is distinct especially for the temperature range below 1600 K as shown in Figure 6, and it is very important for the understanding of the surface processes. Since the rate constants, especially the fast one, vary slowly with temperature below 1600 K, it is apparent that diffusion processes play a role in the removal of K atoms from the surface layer.

The behavior with two independent rate constants in the low-temperature range, below 1560 K, can be explained if several different states are involved in consecutive reaction steps. The reaction sequence at low temperatures is proposed to be

$$\mathrm{K(beam)} \rightarrow \mathrm{K_s^+} \rightarrow \mathrm{K}(\sigma_{4p}) \rightarrow \mathrm{K(4p)} \qquad (17a)$$

$$\mathrm{K}(\sigma_{4p}) \rightleftarrows \mathrm{K}(\sigma_{3d}) + \mathrm{K(3d)} \qquad (17b)$$

(see Figure 4), and the loss of the excited species is then into the graphite or via desorption or transfer to other desorbing species. If the rate of the reaction steps on the surface is small, the number of atoms in the state K_s^+ may be quite significant before the slow conversion to the covalent state σ_{4p} becomes important. In this way, the buildup of the FR peak goes through two stages, one with the filling of the K_s^+ state limited by the rate of transfer to σ_{4p} and subsequent loss, and one with the filling of the σ_{4p} state limited by the rate of transfer to the state σ_{3d} and subsequent loss. The ionic state K_s^+ is not occupied to a large extent owing to the diffusion to the lowest covalent state, and the main desorption and loss into the bulk taking place under retarding field conditions goes via the two covalent states. The excited state flux is likely to cross Rydberg levels after collisions with the surface, and transitions to such levels are then possible. With accelerating field, the desorption from the two covalent states also gives ion emission via the field ionization of Rydberg species outside the surface, and possibly also by transfer to the somewhat ionic 5s state. The fast rate at low temperature is thus identified as corresponding principally to the transfer $K_s^+ \rightarrow \sigma_{4p}$, and the slow rate is identified as corresponding to the transfer $\sigma_{4p} \rightarrow \sigma_{3d}$. The last step is supported by the observation that the slow rate in the range 1220−1560 K even shows a slope of 0.93 eV. This agrees well with the energy difference between the states σ_{4p} and σ_{3d}, which is 0.95 eV in Figure 4.

At temperatures above 1560 K, the fast and slow rates change their appearance radically, as shown in Figure 8. Very large preexponential factors and large activation energies are then found, of almost the same size as in the case of Cs/graphite in refs 20 and 21. This change in mechanism must be due to the elimination of the diffusion steps as the rate-limiting steps, probably since the temperature of the surface is high enough to allow a direct entrance of the beam atoms into the covalent states. As seen in Figure 4, both states are below the level of the impinging ground-state K. The fast rate is then the direct loss process from σ_{4p}, while the slow rate is the loss process from σ_{3d} to high Rydberg states, possibly via K(3d)

$$\mathrm{K(beam)} \rightarrow \mathrm{K}(\sigma_{4p}) \rightarrow \text{desorbed K(4p)} \qquad \text{fast} \quad (18a)$$

$$\mathrm{K(beam)} \rightarrow \mathrm{K}(\sigma_{3d}) \rightarrow \text{desorbed or diffusing K(nl)} \qquad \text{slow} \quad (18b)$$

(see Figure 4) where K(nl) are in high Rydberg states. The two states σ_{3d} and σ_{4p} can now also be transformed directly into each other. The energy levels and the corresponding activation barriers are included in Figure 4 and fit nicely into the overall picture. The values found for the preexponential factors support the loss channels shown above, since the preexponential 6×10^{16} s^{-1} indicates a desorption with higher intermediates (σ_{4p} with the higher σ_{3d} and possibly K_s^+), while the preexponential of close to 10^{21} s^{-1} indicates an electronic switch to a Rydberg state coupled to diffusion into the bulk, as in refs 20 and 21. This will be discussed further below.

At low temperature, the processes follow eq 17. The observed increase of the ratio of the signals indicates that the loss from the state σ_{4p} emptied by the fast process is becoming slower relative to the loss from σ_{3d} at higher temperature. Since the transfer between these two bound states at low temperature is likely to involve the diffusing state K_s^+, the observed activation barrier of 0.68 eV is correctly related to the transfer from σ_{4p} to K_s^+. At high temperature, the direct transfer from the σ_{4p} to σ_{3d} is related to a higher barrier from the ratio betwen the signals, namely, 1.45 eV, while the energy difference between the two states is shown as only 0.95 eV in Figure 4. This may be due to a larger activation barrier for the direct change from the on-top position σ_{4p} to the bridging position of K in σ_{3d}.

This model for the loss and desorption is fully supported by the data for the ionic desorption in the same experiments, shown in Figure 9. Observe that the fast process at high temperature involves loss from the state σ_{4p} with both retarding field (Figure 8) and accelerating field (Figure 9), while the slow process corresponds to loss from the upper state σ_{3d} to high Rydberg states for both field directions.

5.3. Overall Energetics. The largest activation barrier measured in this system is likely to correspond to penetration of an ion K^+ from the lowest bound state in the bulk of the C/Ir material out to the surface. Comparing this value of 7.44 eV to the values found for other systems, it is higher than the value for Cs^+ emission from graphite of 6.0 eV[20,21] and also for K^+ emission from Pt,[35] which is approximately 6.8 eV. However, the total energy difference measured for Cs on graphite between the lowest state at the grain boundaries to the ionization limit outside the surface is 7.18 eV. The difference in ionization energy between the K and Cs, i.e., to the Rydberg states on top of the barrier, is 0.45 eV, which gives a total energy difference value for comparison purposes of 7.63 eV. The difference between the data for K^+ emission from graphite and Pt surfaces[35] is probably real. Thus, the present result for K/C is in agreement with previous results.

Also the various desorption barriers are similar to the case of Cs/C. The barrier for neutral desorption for K is 2.01−0.10 = 1.91 eV according to Figure 4, when the work function of the surface is 0.10 eV lower than the ionization potential. In ref 21 the neutral desorption energy from the highest state of Cs on the surface (initially assumed to be covalent, but later associated with an ionic state) is 2.06 eV. Of course, the ion desorption energies differ considerably owing to the different ionization potentials of K and Cs. The lowest covalent state was in ref 21 found to be between 2.56 and 2.76 eV below the desorbed Cs atom level. In the present case, the lowest covalent state is at an energy of 2.01 + 0.77 = 2.78 eV below the desorbed K level, thus in good agreement with the Cs results. It should be observed that the same type of activation barrier (e.g., from the lowest covalent state to the desorbed atom) cannot always be measured in the two desorption systems of K/C and Cs/C. This is due to the different kinetics caused by different preexponential factors and activation energies. However, the

derived comparison values agree very well, which provides strong support for the kinetic system presented here.

Another interesting point to note in a comparison with Cs/C is that in ref 21 the desorption with no Cs beam was found to have a larger barrier at low temperature than at high temperature, and this was indicated in the potential energy diagrams as a higher state $Cs^+ + e_s^-$, which at high temperature decreased down to the $Cs^+ + e_F^-$ state. This effect was observed at higher field strengths than in the present study but indicates a desorption to a higher state that could be Cs(6p), in analogy to the now observed desorption to the state K(4p).

There exist data in the literature on the desorption of K from C/Ir, in fact from the surface C/Ir(111)[15,27] in the low temperature range 850−1000 K. The neutral desorption energy for K is given as 2.4 ± 0.2 eV. This value should be compared to the desorption from the lowest covalent state to 4s since the electric field strength probably was quite high in the study cited so that the states mixed. The results here give a barrier of 2.68 eV as seen in Figure 4, slightly outside the error limits from refs 15 and 27. An intermixing in the measurements by the ionic state K_s^+ with a desorption energy to 4s of 2.01 eV is possible, which might decrease the desorption energy. The ion desorption energy cited in refs 15 and 27 is 2.2 ± 0.2 eV, which should be compared to the present value of 2.01 eV, thus within the error limits. The preexponential factors were close to 10^{14} s^{-1}, while the values reported now are somewhat smaller. There exists also a report from our group on K desorption from a carbon film on a Pt-8%W surface.[38] Those experiments were done at low temperatures with not so well defined carbon film conditions, at 950−1100 K, below the temperature range studied here. The results were quite variable, with preexponential factors in the range 10^{15}−10^{18} s^{-1}, while the ion desorption energies varied from 2.40 to 2.89 eV. The ion desorption energies are similar to the desorption energy for the lowest covalent state on the surface, shown as 2.78 eV at the low work function of 4.24 eV used in Figure 4, and the agreement with this early study is thus reasonable.

5.4. Very Large Preexponential Factors. A desorption process for an atom or ion in general has a preexponential of the same size as the vibrational frequency. The standard values assumed in many experiments are of the order of 10^{11}−10^{13} s^{-1}. In the case of K atoms and ions, it is known that on most surfaces the preexponential factors are of the order of 10^{13} s^{-1}.[14] The reason for the identification as the vibrational frequency is based on transition-state theory, which means that the atom or ion attempts to leave the surface over a barrier equal to the desorption energy with this frequency. However, the observation of preexponential factors of the order of 10^{21} s^{-1} does not fit into this picture. During a time of 10^{-21} s, the atom or ion moves only 5×10^{-19} m by their thermal energy, and only a fraction 10^{-8} of the vibrational period. Thus, the large preexponential observed cannot be related to a motion of an atom or ion. The period of rotation for an electron around the atom in a Rydberg state is larger than (or much larger than) 10^{-16} s and is thus orders of magnitude too large. Of course, electrons in inner shells have shorter periods of their motion, but they can not be related to a thermal process with a barrier of 6.0 eV.

The process of forming a Rydberg state by recombination of an electron and an ion at the surface is a process that could be thought to give very large preexponential factors. The reason for this would be the large electron density available on the surface. A simple calculation using a large cross section for recombination of 10^4 Å^2 still gives a preexponential of only 10^{15} s^{-1}. Thus, no recombination process seems to be able to give the preexponential of 10^{21} s^{-1}. On the other hand, the preexponential of 6.2×10^{16} s^{-1} observed at high temperatures for the fast rate may be related to a Rydberg formation and desorption process, as already concluded from the barrier value.

Using the uncertainty relation, the uncertainty in energy related to an uncertainty in time of 10^{-21} s is of the order of 10^5 eV. This means that any electronic transition is possible to match this short time, and it is thus very likely that the process with the preexponential of 10^{21} s^{-1} is an electronic excitation process, i.e., a thermally excited electronic excitation process with an excitation energy of 6.08 eV. This process may be coupled to an excitation process in the graphite layer, enabling a subsequent diffusion of the atom into the bulk, as proposed previously.[13]

It is also notable that the large energy barrier for penetration into the bulk on a graphite/Ir surface was observed independently in ref 39. The authors observed an activation energy of 5.5 eV, which they attributed to diffusion into the bulk from a position below the first graphite monolayer on the Ir surface. They also state that the lifetime of the K atoms on the surface is very long, 200 s at 1800 K. They do not measure the preexponential factor but assume it to be 10^{13} s^{-1}. However, we show directly that the lifetime on the surface is short at this temperature, of the order of 1 μs, and that the large energy barrier is coupled directly to the process of loss from the surface, not belonging to a second step for diffusion into the bulk. We also show directly that the preexponential factor is in the range 10^{16}−10^{21} s^{-1} for the various processes resolved.

In a recent study of K desorption and diffusion on the basal face of a graphite crystal,[13] the fast diffusion with retarding field conditions into the graphite surface was observed also in the temperature range 1000−1500 K, i.e., where the present study primarily detects the diffusion processes between the various states on the surface. The step following the diffusion steps is excitation and loss from the surface via desorption or diffusion into the surface, according to eq 17. The diffusion steps are thus observed in the present kinetic study, while the final loss from the surface is observed in ref 13.

6. Conclusions

The kinetics of desorption and loss for K atoms on a graphite-covered Ir surface has been investigated in detail. This system is of great interest since Rydberg states of K are reported to desorb thermally under a variety of conditions. The rapid field reversal kinetics method combined with molecular beam dosing makes it possible to study the neutral kinetics over a very large temperature range, and at much higher temperatures than previously. The results show that three adsorbed states exist on the surface, two covalent and one ionic. At high temperature, processes with extremely large preexponential factors (10^{21} s^{-1} instead of normally 10^{13} s^{-1}) are observed, which are due to electronic excitation processes. There are several reasons why Rydberg states are formed at graphite surfaces: (a) covalent bound states exist that do not give ions in desorption, (b) the ground-state 4s is not reached directly by desorption from a stable adsorbed state, (c) the covalent bound states give excited states in desorption, and (d) these excited states can be transferred to Rydberg states by thermal processes on the surface.

References and Notes

(1) *Rydberg States of Atoms and Molecules*; Stebbings, R. F., Dunning, F. B., Eds.; Cambridge University Press: Cambridge, 1983.

(2) Gallagher, T. F. *Rydberg Atoms*; Cambridge University Press: Cambridge, 1994.
(3) Pettersson, J. B. C.; Holmlid, L. *Surf. Sci.* **1989**, *211*, 263.
(4) Lundin, J.; Engvall, K.; Holmlid, L.; Menon, P. G. *Catal. Lett.* **1990**, *6*, 85.
(5) Åman, C.; Pettersson, J. B. C.; Holmlid, L. *Chem. Phys.* **1990**, *147*, 189.
(6) Wallin, E.; Hansson, T.; Holmlid, L. *Int. J. Mass Spectrom. Ion Processes* **1992**, *114*, 31.
(7) Holmlid, L.; Pettersson, J. B. C.; Åman, C.; Lönn, B.; Möller, K. *Rev. Sci. Instrum.* **1992**, *63*, 1966.
(8) Holmlid, L.; Pettersson, J. B. C.; Hansson, T.; Wallin, E. *Rev. Sci. Instrum.* **1994**, *65*, 2034.
(9) Åman, C.; Holmlid, L. *Appl. Surf. Sci.* **1992**, *62*, 201; **1993**, *64*, 71.
(10) Engvall, K.; Kotarba, A.; Holmlid, L. *Catal. Lett.* **1994**, *26*, 101.
(11) Holmlid, L. *Z. Phys. D* **1995**, *34*, 199.
(12) Andersson, M.; Wang, J.; Holmlid, L. *J. Chem. Soc., Faraday Trans.* **1996**, *92*, 4581.
(13) Holmlid, L.; Wang, J. *Chem. Phys. Lett.* **1997**, *268*, 285.
(14) Zandberg, E. Ya.; Ionov, N. I. *Surface Ionization* (translated from Russian); Israel Program for Scientific Translations: Jersusalem, 1971.
(15) Nazarov, E. G.; Rasulev, U. Kh. *Nonstationary process of surface ionization*; FAN Academy of Science: Tashkent Uzbekistan, 1991 (in Russian).
(16) Holmlid, L.; Olsson, J. O. *Rev. Sci. Instrum.* **1976**, *47*, 1167.
(17) Holmlid, L.; Olsson, J. O. *Surf. Sci.* **1977**, *67*, 61.
(18) Holmlid, L.; Lönn, B.; Olsson, J. O. *Rev. Sci. Instrum.* **1981**, *52*, 63.
(19) Zazula, P. *Ark. Fys.* **1968**, *38*, 97.
(20) Möller, K.; Holmlid, L. *Surf. Sci.* **1988**, *204*, 98.
(21) Möller, K., Holmlid, L. *Surf. Sci.* **1986**, *173*, 264.
(22) Hansson, T.; Pettersson, J. B. C.; Holmlid, L. *Surf. Sci.* **1991**, *253*, 345.
(23) Möller, K.; Holmlid, L. *Surf. Sci. Lett.* **1985**, *163*, L635.
(24) Bauer, M.; Pawlik, S.; Aeschlimann, M. *Phys. Rev. B.* **1997**, *55*, 10040.
(25) Taylor, J. B.; Langmuir, I. *Phys. Rev.* **1933**, *44*, 423.
(26) Kaminsky, M. *Atomic and Ionic Impact Phenomena on Metal Surfaces*; Springer: Berlin, 1965.
(27) Tontegode, A. Ya. *Prog. Surf. Sci.* **1991**, *38*, 201.
(28) Kupriyanov, S. E. *JETP Lett.* **1967**, *5*, 197.
(29) Fabre, C.; Gross, M.; Raimond, J. M.; Haroche, S. *J. Phys. B.* **1983**, *16*, L671.
(30) Kocher, C. A.; Taylor, C. R. *Phys. Lett. A.* **1987**, *124*, 68.
(31) McCown, G. E.; Taylor, C. R.; Kocher, C. A. *Phys. Rev A* **1988**, *38*, 3918.
(32) Kocher, C. A.; McCown, G. E. *Surf. Sci.* **1991**, *244*, 321.
(33) Zeman, H. D. *Rev. Sci. Instrum.* **1977**, *48*, 1079.
(34) Holmlid, L.; Olsson, J. O. *Surf. Sci.* **1976**, *55*, 523.
(35) Möller, K.; Holmlid, L. *Surf. Sci.* **1987**, *179*, 267.
(36) Holmlid, L. *Chem. Phys.* **1998**, *230*, 327.
(37) Nordholm, S. *Chem. Phys.* **1985**, *98*, 367.
(38) Olsson, J. O.; Holmlid, L. *Mater. Sci. Eng.* **1980**, *42*, 121.
(39) Tontegode, A. Ya., Yusifov, F. K. *Phys. Solid State* **1993**, *35*, 506.